

Simulation Model of *Skeletonema costatum* Population Dynamics in Northern San Francisco Bay, California

James E. Cloern and Ralph T. Cheng

U.S. Geological Survey, 345 Middlefield Road, Menlo Park, California 94025, U.S.A.

Received 19 October 1979 and in revised form 31 March 1980

Keywords: phytoplankton; ecology; population dynamics; primary production; estuarine circulation; San Francisco Bay

A pseudo-two-dimensional model is developed to simulate population dynamics of one dominant phytoplankton species (*Skeletonema costatum*) in northern San Francisco Bay. The model is formulated around a conceptualization of this estuary as two distinct but coupled subsystems—a deep (10–20 m) central channel and lateral areas with shallow (<2 m) water and slow circulation. Algal growth rates are governed by solar irradiation, temperature and salinity, while population losses are assumed to result from grazing by calanoid copepods. Consequences of estuarine gravitational circulation are approximated simply by reducing convective-dispersive transport in that section of the channel (null zone) where residual bottom currents are near zero, and lateral mixing is treated as a bulk-exchange process between the channel and the shoals.

Model output is consistent with the hypothesis that, because planktonic algae are light-limited, shallow areas are the sites of active population growth. Seasonal variation in the location of the null zone (a response to variable river discharge) is responsible for maintaining the spring bloom of neritic diatoms in the seaward reaches of the estuary (San Pablo Bay) and the summer bloom upstream (Suisun Bay). Model output suggests that these spring and summer blooms result from the same general process—establishment of populations over the shoals, where growth rates are rapid, coupled with reduced particulate transport due to estuarine gravitational circulation. It also suggests, however, that the relative importance of physical and biological processes to phytoplankton dynamics is different in San Pablo and Suisun Bays. Finally, the model has helped us determine those processes having sufficient importance to merit further refinement in the next generation of models, and it has given new direction to field studies.

Introduction

Many of the world's largest estuaries are sites of concentrated urban/industrial activity as well as productive aquatic ecosystems that can support fisheries having commercial and recreational value. Because estuaries have ecological and economic importance, and because they are often subjected to extreme natural and man-related stresses, there is need to understand those interactions between the physical, chemical, geological and biological processes

that determine their water quality and productivity. Our understanding of estuaries as ecological systems requires a knowledge of factors that regulate phytoplankton productivity and biomass, since phytoplankton dynamics govern other dynamic properties of the water column (e.g. transparency, concentration of nutrients, dissolved O_2 and CO_2 , and particulate and dissolved organic matter, secondary productivity). This paper describes a numerical model that simulates population dynamics of one dominant phytoplankton species in the northern San Francisco Bay estuary. The model was developed to: (i) test hypotheses concerning mechanisms that regulate phytoplankton biomass in this estuary, (ii) provide initial estimates of the relative magnitudes of individual processes governing phytoplankton dynamics there, (iii) assist in the planning of field studies, and (iv) lay a foundation for long-term development of realistic ecosystem models.

Most existing models of estuarine ecosystems (e.g. Chen & Orlob, 1975; Kelley, 1976; DiToro et al., 1977) treat the phytoplankton as a homogeneous assemblage. However, estuarine phytoplankton communities can be extremely diverse, ranging from freshwater assemblages at the estuary head to marine assemblages at the mouth. Since each assemblage responds differently to environmental variations (salinity, temperature, solar irradiance and nutrient concentrations), the assumption of homogeneity among estuarine phytoplankton is often a crude approximation that may lead to invalid conclusions from simulation models. Therefore, we chose to incorporate physiologically-realistic growth kinetics of one dominant species, rather than treat the phytoplankton as a homogeneous unit. The intention was to develop a realistic monospecific model, with the expectation that generalities from this particular model will further our knowledge about phytoplankton dynamics in general.

San Francisco Bay

San Francisco Bay, California, is a complex system comprising two distinct but connected estuaries [see Conomos (1979) for a detailed description]. The South Bay is a large embayment that receives only small inputs of freshwater from local runoff and sewage effluent. The northern reach is a partially mixed estuary that links California's two longest rivers, the Sacramento and San Joaquin, to the Pacific Ocean (Figure 1). The northern reach has been the subject of considerable study recently (Conomos, 1979); this research has been directed primarily toward assessing the impacts of past and proposed future diversions of freshwater and is partly motivated by a concern for the valuable striped bass (*Morone saxatilis*) fishery supported by the estuary (Stevens, 1979). We have concentrated initial modeling efforts on this northern reach where sufficient data exist to permit development of preliminary models.

The primary source (>90%) of freshwater to northern San Francisco Bay is the Sacramento-San Joaquin River system that passes through a series of leveed islands and sloughs (the Delta). A relatively deep (10–20 m) and narrow channel occupies the central region, and lateral to this channel is a series of shallow embayments (San Pablo Bay, Grizzly Bay and Honker Bay, Figure 1) which have mean depth less than 2 m. Annual variations in the distributions of salinity, temperature, and suspended sediment in the estuary are closely coupled to variations in freshwater discharge through the Sacramento-San Joaquin Delta. Discharge typically varies between about 1×10^7 and 2×10^8 m^3 day^{-1} (Peterson et al., 1975a), is maximal in late winter to early spring, minimal during late summer, and variable during fall [e.g. Figure 2(a)]. Empirical functions [Figure 2(b)–(d)], based upon 7 years of field study (Smith et al., 1979), represent mean spatial and seasonal variations of salinity, temperature and turbidity (measured as light extinction coefficient ϵ). Surface salinity typically varies from an annual minimum of about 25‰ to an annual maximum of

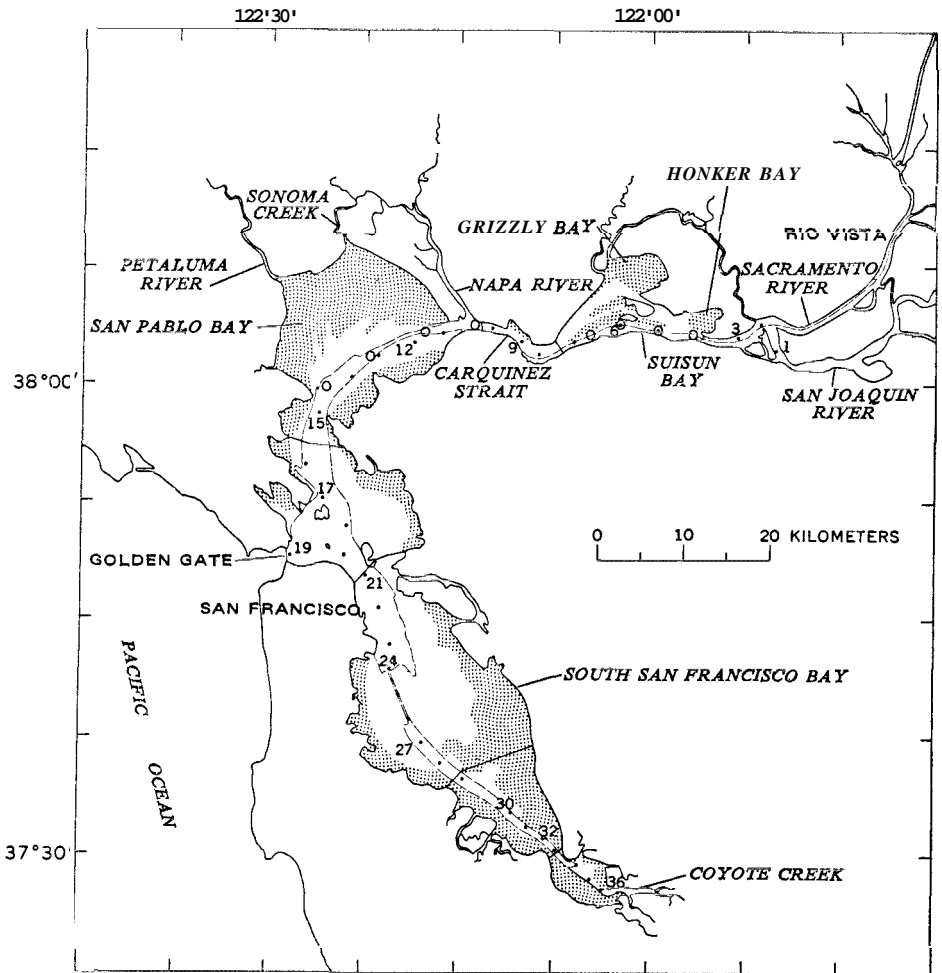


Figure 1. Map of San Francisco Bay showing location of U.S. Geological Survey sampling stations (solid circles) and stations (open circles) where samples were collected for phytoplankton enumeration (Storrs *et al.*, 1964). Gray stipple demarcates shoal areas (MTL depth ≤ 2 m); dashed line represents the central shipping channel (10-m isobath).

about 33‰ at the seaward extent of the northern reach (defined here as Station 17—Figure 1). Salinity at a position just west of the Delta (Station 3) varies between 0.1‰ and about 6‰ [Figure 2(b)]. Annual variations in temperature [Figure 2(c)] are most extreme in the landward reaches of the estuary, varying from about 8 °C to 22 °C; the seaward boundary experiences a smaller annual variation in temperature, from about 11 °C to 17 °C. Suspended sediment load and turbidity decrease from the Delta toward Golden Gate, and increase with increasing river discharge [Figure 2(d)]. During summer, daily irradiance is higher in landward portions of the northern reach because of morning fog and overcast near the Pacific Ocean [Figure 2(e)].

Two different patterns of temporal variation in phytoplankton standing crop are seen within the northern reach. Whereas San Pablo Bay has maximum standing crops during late

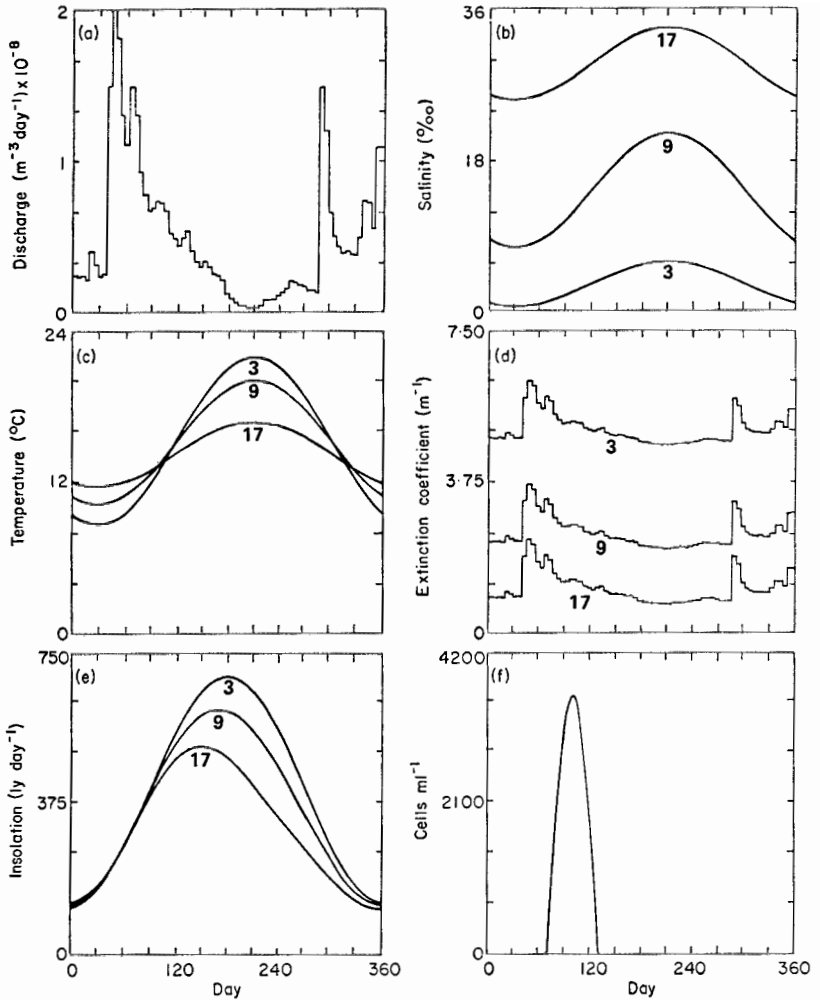


Figure 2. (a) Five-day mean values of discharge (USBR, Sacramento, California) through the Sacramento–San Joaquin Delta during 1962, and empirical functions describing mean seasonal variations in (b) salinity, (c) temperature, (d) extinction coefficient and (e) daily surface insolation at the seaward (Station 17), middle (Station 9) and landward (Station 3) reaches of northern San Francisco Bay. Frames (b)–(d) are based upon data of Smith *et al.* (1979); frame (e) is based upon data from the Bay Area Air Pollution Control District. (f) Also shown is the boundary condition of *S. costatum* population density specified at Station 17 in the simulation model.

spring–early summer, Suisun Bay has maximum phytoplankton densities in late summer–early fall (Cloern, 1979); during some years, Suisun Bay also has a spring phytoplankton bloom (Ball & Arthur, 1979). The few published studies of phytoplankton composition (Storrs *et al.*, 1966; U.S. Bureau of Reclamation, 1976) suggest that neritic diatoms dominate the spring and summer blooms, with *Skeletonema costatum* accounting for roughly half (up to 99%; Ray Wong, personal communication) of the algal cells present during blooms.

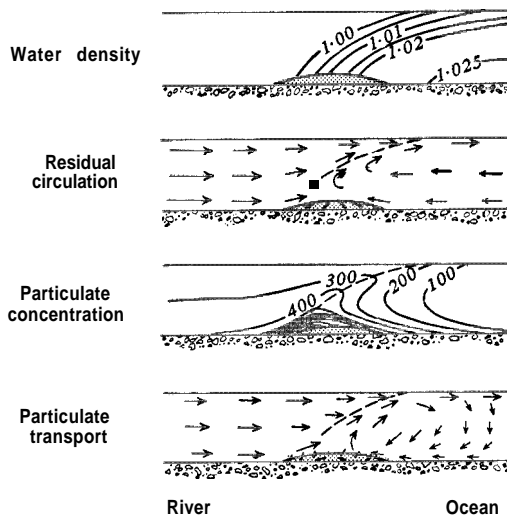


Figure 3. Spatial variations of water density, residual circulation, concentration of suspended particulates and net transport of particulates within the null zone of a partially mixed estuary [redrawn from Meade (1972)].

Model development

Conceptual model

We conceptualize the northern reach of San Francisco Bay as two distinct but closely coupled subsystems—the deep channel and the expansive shallows adjacent to the channel (Figure 1). Tidal-current charts (Coast and Geodetic Survey, 1964) and hydrodynamic models (Walters & Cheng, 1979) indicate that circulation is relatively strong in the channel but weak over the shallows. Temporal variations in the distribution of many properties (e.g. suspended particulates, dissolved nutrients) along the channel are regulated by seasonal variations in river flow (Peterson et al., 1975a; Conomos, 1979). Seasonal variations in discharge have a particularly strong influence on the distribution of dense particulates (including diatoms) since the transport of suspended particulates is governed by estuarine gravitational circulation (Conomos & Peterson, 1977; Arthur & Ball, 1979). As dense particulates are carried downstream in the surface layer, they settle and merge into the landward-flowing bottom density current which transports them upstream (Postma, 1967; Meade, 1972; Figure 3). Consequently, dense particles accumulate in that part of the estuary ('null zone') where residual (tidally-averaged) bottom currents balance convective currents from river flow. An impact of estuarine circulation, then, is a significant reduction in the net transport of particulates by convection–dispersion near the null zone. Seasonal variations in the location of the null zone, a response to variable river discharge (Peterson et al., 1975b), thus partly explain the spring diatom bloom in San Pablo Bay and summer bloom in Suisun Bay, since the null zone is located seaward during high discharge of spring and moves landward during the summer period of low river flow.

In addition to the consequences of estuarine gravitational circulation, we hypothesize that spatial variations in the growth rate of planktonic algae play a critical role in regulating phytoplankton biomass. Algal growth rates are governed by a complex interaction between water chemistry (including salinity and concentrations of nutrients and toxins), light availability and temperature. Nutrients (N, P, Si) rarely approach rate-limiting concentrations

TABLE 1. Median (range) concentrations ($\mu\text{mol l}^{-1}$) of dissolved Si, NH_4 , $\text{NO}_3 + \text{NO}_2$, and P in Suisun Bay (Station 6) during winter (December–April) and summer (July–October) 1969–1977 [data from Conomos *et al.* (1979)]

	Winter	Summer
Si	257 (203–389)	119 (47–207)
NH_4	4.0 (1.6–9.2)	1.8 (0.4–5.7)
$\text{NO}_3 + \text{NO}_2$	21.9 (15.9–27.0)	7.3 (2.3–15.5)
P	2.0 (1.2–3.1)	2.4 (1.7–3.4)

in northern San Francisco Bay (Peterson & Conomos, 1975; Table 1), and *in-situ* measures of primary productivity (Cole & Herndon, 1979) suggest that phytoplankton populations are not stressed greatly by toxins. Therefore, growth rates of planktonic algae (including *S. costatum*) are governed primarily by light availability, salinity, and temperature. Concentrations of suspended particulates in the northern reach [Figure 2(d)] are such that the vertically-mixed water column of the deep (>10 m) channel does not have sufficient light to support algal photosynthesis and cell division in Suisun Bay. Although the shoals are generally more turbid than the channel, light availability in their shallow water column is sufficient to support net photosynthetic carbon assimilation and cell division (Cloern, 1978). We hypothesize, then, that two factors are responsible for the seasonal distribution of *S. costatum* (and other neritic diatoms): (i) estuarine circulation, a physical process that accumulates diatoms and other particulates in the null zone, and (ii) positioning of the null zone next to productive shallow areas where light availability is sufficient to support population growth. Causes of phytoplankton population decline are poorly understood, but zooplankton grazing is probably the major cause of loss.

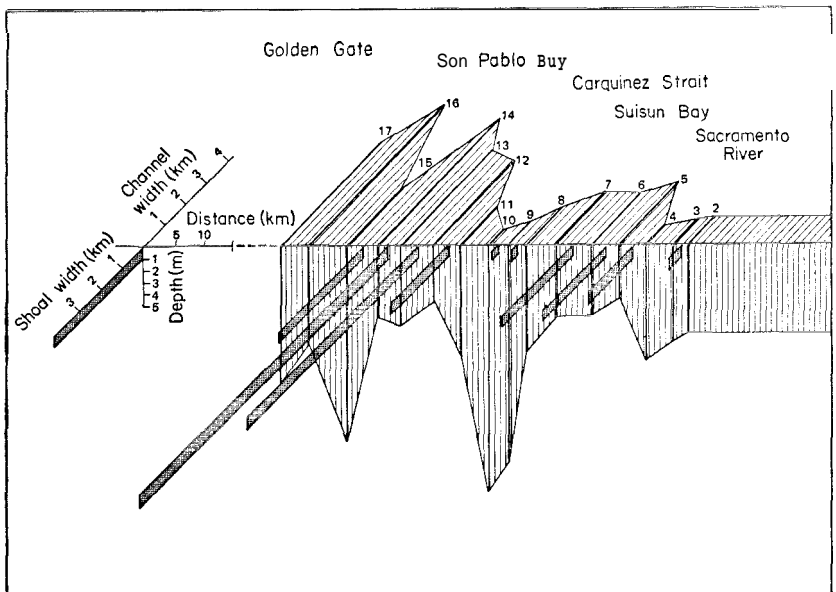


Figure 4. Schematic diagram showing dimensions of the discrete channel and shoal segments used to approximate the geometry of northern San Francisco Bay. Also shown are computational nodes (numbered stations) used in the finitedifference approximation of equation 1.

Mathematical model

The primary objective of this study was to develop a model to simulate changing phytoplankton biomass, along the longitudinal axis of the estuary channel, over moderate time scales (days) and large spatial scales (kilometers). It was necessary, then, to utilize governing equations that average out processes occurring over short time scales (e.g. tidal-cycle). Vertical and lateral variations in phytoplankton biomass within the channel are normally small, but lateral gradients between the channel and shoals are large (Cloern, 1979). We approximated the entire system in a pseudo-two-dimensional manner by treating the channel as a vertically and laterally homogeneous, segmented system that exchanges material across an interface with segments of the well-mixed, shallow embayments (Figure 4). The complex process of lateral mixing, resulting primarily from tidal circulation, was approximated in a manner analogous to Ketchum's (1950) treatment of estuarine flushing by tidal mixing.

The distribution of phytoplankton population density (P) in the channel was represented by the one-dimensional convection–dispersion equation that is tidally and cross-sectionally averaged (Harleman, 1971), with an additional term accounting for lateral mixing with the shoals [see Ketchum (1950) and Chapra (1979) for similar formulations]:

$$\underbrace{\frac{\partial P}{\partial t}}_{\text{time rate of change of } P} = \underbrace{-u \frac{\partial P}{\partial x}}_{\text{convective flux}} + \underbrace{E \frac{\partial^2 P}{\partial x^2}}_{\text{longitudinal dispersion}} + \underbrace{(\mu - d)P}_{\text{growth and loss rate}} + \underbrace{K(P_s - P)}_{\text{exchange with the shoals}}, \quad (1)$$

where P has units cells ml^{-1} , t is time (days), x is distance (m) along the channel east of Golden Gate, u is residual convective velocity (m day^{-1}), μ and d are specific rates of growth and death (days^{-1}), K is a bulk exchange coefficient between the channel and shoals (days^{-1}) and P_s is population density in the adjacent shoals. Processes of longitudinal transport and population growth in the channel were solved in finite difference form (see below) using a spatial discretization of the northern reach (Figure 4) where computational nodes correspond to U.S. Geological Survey stations. Phytoplankton dynamics in the shoals are governed by two processes, net population growth and lateral exchange with the channel:

$$\underbrace{\frac{\partial P_s}{\partial t}}_{\text{time rate of change of } P_s} = \underbrace{(\mu_s - d_s) P_s}_{\text{growth and loss rates over the shoals}} - \underbrace{K_s (P_s - P)}_{\text{exchange with the channel}}, \quad (2)$$

where μ_s and d_s are specific rates of growth and death in the shoals, and K_s is a coefficient to quantify the exchange of material from shoals to the channel. As explained below, the bulk exchange coefficient K_s is a scaled value of K , where the scaling factor is the ratio of water volume over the shoals to volume of the channel (Figure 5).

Convection and dispersion in the channel. Convective velocity u , representing the net residual currents, was computed simply as discharge through the Sacramento–San Joaquin Delta, Q ($\text{m}^3 \text{day}^{-1}$), divided by the channel cross-sectional area A (m^2):

$$u(x) = \frac{Q}{A(x)} \quad (3)$$

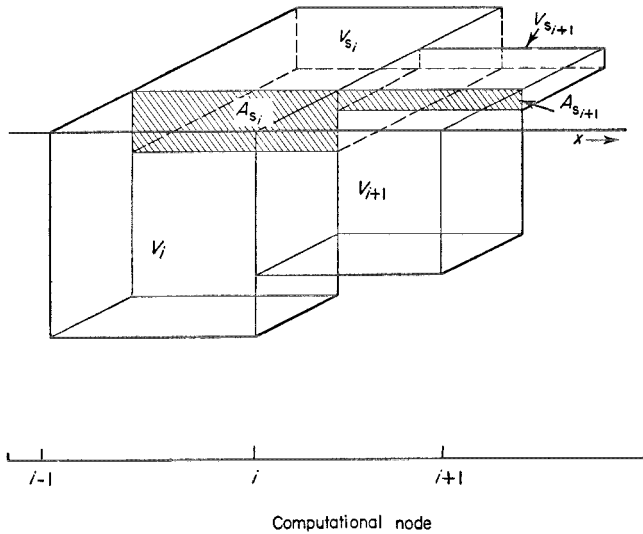


Figure 5. Schematic diagram showing two adjacent channel and shoal segments along the longitudinal (x) axis of the estuary. Lateral to each channel segment, having volume V , is a shoal segment having volume V_s ; channel and shoal segments are connected by a common cross-sectional area A_s .

Glenne & Selleck (1969) estimated values of the longitudinal dispersion coefficient (E) by fitting observed distributions of chlorosity and silicate concentration to the convection-dispersion equation. They observed that estimated values of E were consistently higher in the vicinity of San Pablo Bay than near Suisun Bay, and increased with increasing convective velocity. Their measured values of E in San Pablo and Suisun Bays were fit separately to functions of u :

$$\begin{aligned} E(x) &= (1.44 \times 10^6) u^{0.48} & 0 \leq x_i \leq 45\,700 \\ E(x) &= (0.13 \times 10^6) u^{0.65} & 45\,700 < x_i, \end{aligned} \quad (4)$$

where x_i is distance of the i -th station from Golden Gate and $x_0 = 45\,700$ m is where Carquinez Strait separates San Pablo Bay from Suisun Bay (Figure 4).

In-situ growth and death rate. Growth rate of *Skeletonema costatum* was estimated from an empirical model (Cloern, 1978) that defines photosynthetic rate as a function of water temperature (T), salinity (S), surface irradiance (I), turbidity (ϵ), depth of the water column (H) and photoperiod (λ). The model is based upon a modification of Steele's (1965) function of irradiance:

$$P_{\text{net}}(I) = P^* \frac{I}{I_{\text{opt}}} \exp\left(1 - \frac{I}{I_{\text{opt}}}\right) - a, \quad (5)$$

where P_{net} is net photosynthetic rate ($\text{pg C cell}^{-1} \text{h}^{-1}$) at irradiance I ($\text{ly h}^{-1} \text{PAR}$), P^* is a maximum rate that occurs at irradiance I_{opt} , and a is a basal rate of excretory/respiratory carbon loss ($\text{pg C cell}^{-1} \text{h}^{-1}$). Each of the parameters in equation 5 varies with temperature T : P^* and I_{opt} increase nearly-exponentially up to a maximum at 26°C ; a is an exponential function of temperature (Cloern, 1978). The response of *S. costatum* to variations in salinity was approximated by the function:

$$f(S) = \frac{(S-3.8)}{15.7} \exp\left(1 - \frac{(S-3.8)}{15.7}\right), \quad (6)$$

where $f(S)$ is a reduction factor (fraction of maximum photosynthetic rate) that equals one at the optimum salinity (19.5‰) and declines as salinity deviates from this optimum.

Equations (5) and (6) predict net photosynthetic rate at any depth in a water column and any time of day if depth and diurnal variations of irradiance are defined. We assumed a constant coefficient of light attenuation ε , giving depth variations in irradiance:

$$I(z, \tau) = I_s(\tau) \exp(-\varepsilon z), \quad (7)$$

where z is depth (m), τ is time (hour of day), ε is extinction coefficient (m^{-1}), and $I_s(\tau)$ is surface insolation approximated by Vollenweider's (1965) function:

$$I_s(\tau) = \frac{I_s^*}{2} \left[1 + \cos\left(\frac{2\pi(\tau - 12)}{\lambda}\right) \right] \quad (8)$$

where I_s^* is surface irradiance (ly h^{-1}) at noon and λ is photoperiod (h). Then mean daily carbon assimilation ($\bar{P} = \text{pg C cell}^{-1} \text{ day}^{-1}$) in a water column of depth H (m) is:

$$\bar{P} = \frac{1}{H} \int_0^{24} \int_0^H \left[f(S) P^*(T) \frac{I(z, \tau)}{I_{\text{opt}}(T)} \exp\left(1 - \frac{I(z, \tau)}{I_{\text{opt}}(T)}\right) - \alpha(T) \right] dz d\tau. \quad (9)$$

Although equation (9) cannot be integrated analytically, the double integral does have a simple series solution that converges rapidly [see Cloern (1978) for a derivation].

Assuming that mean carbon quota (q_c) of *S. costatum* is 20 pg C cell $^{-1}$ (McAllister *et al.*, 1964; Eppley & Sloan, 1965; Jorgensen, 1968), then specific growth rate is given by:

$$\mu = \frac{\bar{P}}{q_c}, \quad (10)$$

where \bar{P} was computed from equation (9), using input values of temperature, salinity, extinction coefficient, total insolation (Figure 2) and depth of the channel and shoals (Figure 4). We assumed that photosynthetically available radiation is 0.5 times total solar radiation, and that extinction coefficient of water over the shoals is 1.25 times extinction coefficient in the channel [a mean value from U.S. Bureau of Reclamation *et al.*, (1977)].

In addition to carbon losses from respiration [equation (5)], losses of *S. costatum* were assumed to be a result of zooplankton grazing, where dominant zooplankters in the northern reach are two calanoid copepods of similar size, *Acartia clausi* and *Eurytemora affinis* (Painter, 1966). Although ingestion rate of these copepods is a complex function of particle (detritus, phytoplankton, and microzooplankton) density and size distribution (Richman *et al.*, 1977), we approximated algal losses to grazers by assuming that each copepod effectively filters 0.007 l day $^{-1}$ [this is a mean value inferred from the studies of Nival & Nival (1976), Conover (1956) and O'Connors *et al.* (1976)]. Then specific loss rate of *S. costatum* is simply filtration rate times zooplankton density Z (copepods l $^{-1}$).

$$d = 0.007 Z. \quad (11)$$

Zooplankton density was described by simple functions (see below) fit to measured copepod densities (Storrs *et al.*, 1963, 1964) in San Pablo and Suisun Bays during 1962 (Figure 6). Zooplankton density in the shallows of San Pablo Bay was assumed to be 1.5 times their density in the adjacent channel [a mean value from Painter (1966)].

Lateral exchange between channel and shoals. The last term of equation (1) accounts for mass transport of material across the channel/shoal boundary. This formulation derives from the assumption that material flux across the interface is directly proportional to the difference in phytoplankton population density between a shoal segment and adjacent channel segment. The coefficients K and K_s quantify unidirectional transport of phytoplankton, and are defined as:

$$K = \frac{\alpha_s A_s}{V} \quad (12)$$

$$K_s = \frac{\alpha_s A_s}{V_s}, \quad (13)$$

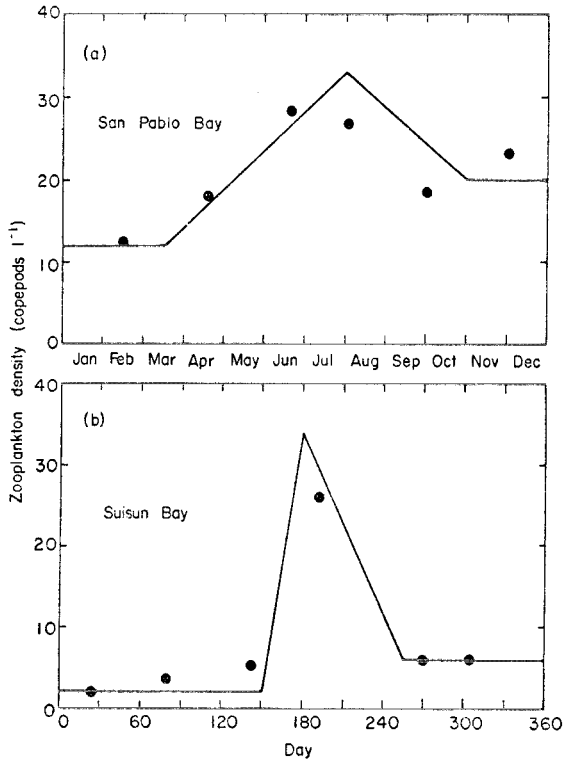


Figure 6. Mean population density of copepods in San Pablo Bay (a) and Suisun Bay (b) during 1962 [from Storrs *et al.* (1963, 1964)].

where α_s is an effective exchange velocity (m day^{-1}), A_s is cross-sectional area (m^2) common to a channel and shoal segment (Figure 5), V_s and V are volumes (m^3) of shoal and channel segments as defined in Figure 4. The lateral exchange velocity α_s was assumed to be constant, and was estimated numerically by picking that value (3750 m day^{-1}) that permitted the ratio P_s/P to reach, but not exceed, two. This is consistent with field observations that mean phytoplankton biomass over shallow areas is roughly double that in the adjacent channel (U.S. Bureau of Reclamation *et al.*, 1977).

Estuarine gravitational circulation. Realistic description of particulate transport within an estuarine circulation cell requires vertical, two-dimensional hydrodynamic and transport

models. Although this transport mechanism is complex, its net effect is simply to reduce the convective-dispersive displacement of heavy particles. We therefore approximated this mechanism by reducing calculated values of u and E within a 10-km segment of the channel defined as the null zone. Convective velocity u was set to zero and values of E were reduced by a factor of 0.9 in the null zone; this reduction produced simulations that match closely the longitudinal distribution of phytoplankton biomass in the channel of San Pablo and Suisun Bays (e.g. Cloern, 1979). Location of the null zone center varies nearly linearly with river discharge (Figure 7), and was positioned near San Pablo Bay during high discharge of spring and in Suisun Bay during summer (Peterson *et al.*, 1975*b*).

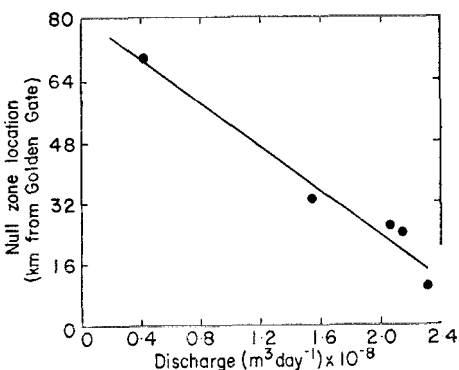


Figure 7. Position of the null zone (distance east of Golden Gate) as a linear function of net discharge through the Sacramento-San Joaquin Delta [based upon data of Peterson *et al.* (1975*b*)].

Method *g* solution. Population densities of *S. costatum* were simulated in northern San Francisco Bay over an annual cycle representative of 1962, starting with initial conditions of 10 cells ml^{-1} for all x_i on Julian day 1. At the seaward boundary of the northern reach (Station 17), the density of *S. costatum* was specified as a large spike centered around day 110 [Figure 2(f)]. This boundary condition was picked to fit measured densities in San Pablo Bay during the spring of 1962, and is consistent with the hypothesis that population development of neritic diatoms inside Golden Gate is initiated by input of allochthonous populations derived from coastal water [see Cloern (1979)]. The landward boundary was specified as a location in the Sacramento River, arbitrarily fixed at 100 km from Golden Gate, where population density of *S. costatum* is always zero.

Because our treatment of lateral transport (bulk exchange across an interface) has a different characteristic time scale than longitudinal transport (convection and dispersion), we utilized a numerical scheme that solves equation (1) in two steps. During the simulation, population densities in the channel were first incremented over time step Δt (0.25 days) by solving the finite difference analog of the convection-dispersion equation (equation 1 minus the last term, which represents lateral exchange), using the Crank-Nicholson method (McCracken & Dorn, 1964), at spatial nodes shown in Figure 4. Between time steps Δt , a cycle was initiated to solve for lateral transport and population growth in the shoals. This was accomplished by calculating the change of P due to the last term of equation (1) ($\partial P / \partial t = K(P_s - P)$) and equation 2 alternately. In finite difference form, using a time step of 0.1 Δt , these equations become

$$P(t + 0.1\Delta t) = P(t) + [K(P_s - P)] [0.1\Delta t], \quad (14)$$

$$P_s(t + 0.1\Delta t) = P_s(t) + [(\mu_s - d_s) P_s - K_s(P_s - P)] [0.1\Delta t]. \quad (15)$$

The small time step used for the lateral transport process was required to maintain conservation of mass.

The model was calibrated to fit measured population densities of *S. costatum* in the channel of mid-San Pablo Bay and Suisun Bay during 1962 (Storrs *et al.*, 1964). After the boundary condition [Figure 2(f)] was specified to initiate the spring bloom in San Pablo Bay, subsequent calibration was effected by adjusting (i) the degree of transport reduction in the null zone and (ii) the linear functions used to define zooplankton abundance (Figure 6). Both simulated and observed populations grew rapidly in San Pablo Bay during early spring, then declined to low levels in mid-summer, and increased slightly during late summer–early fall [Figure 8(a)]. Simulated and observed populations in Suisun Bay exhibited a converse pattern, with a small spring increase followed by an early summer minimum and then a late summer maximum [Figure 8(b)].

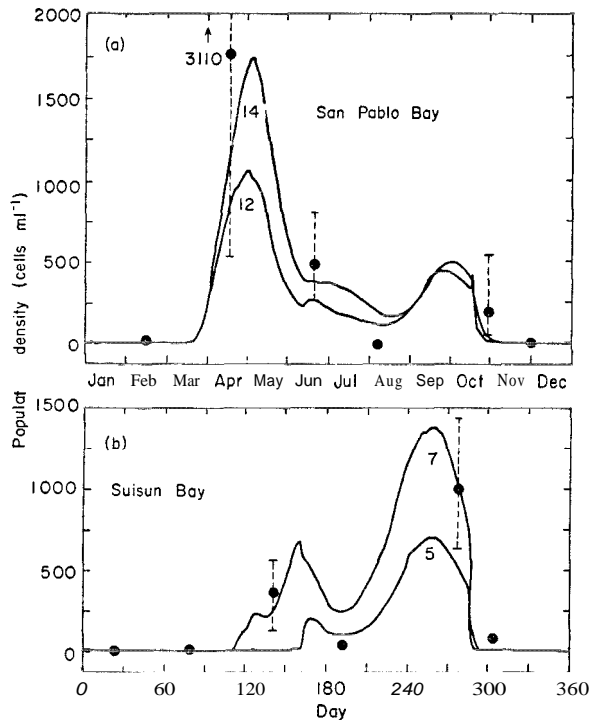


Figure 8. Simulated (solid line) and measured densities of *S. costatum* in the channel of mid-San Pablo Bay (a; Stations 12 and 14) and mid-Suisun Bay (b; Stations 5 and 7) during 1962. Measured densities (Storrs *et al.*, 1964) represent the mean (circles) and range (dashed line) of four samples (near-surface and near-bottom samples at higher high and lower low tides) collected at each of four stations (see Figure 1).

Discussion

Because this model simulates observed temporal changes in *Skeletonema costatum* abundance (particularly the small spring and large summer blooms in the Suisun Bay Channel), is

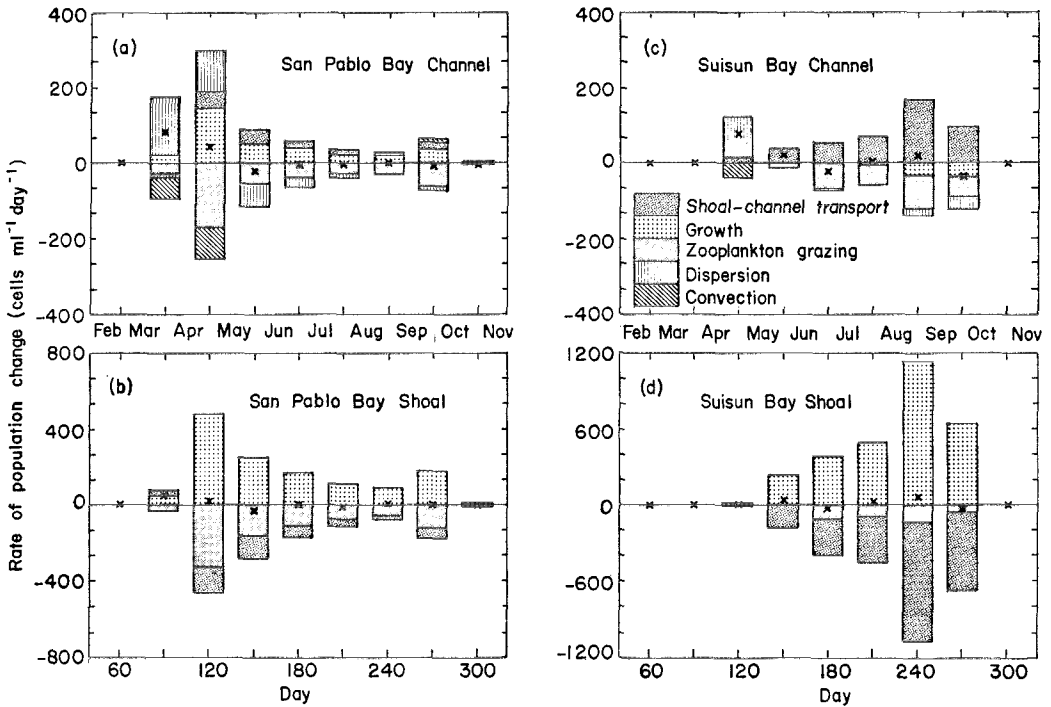


Figure 9. Computed magnitude of each process affecting population density of *S. costatum* in mid-San Pablo Bay (Station 13) and mid-Suisun Bay (Station 6) channel and shoals, at nine times of the simulated year; also shown is the net rate of population change (x). Note the scale differences between channel and shoals.

consistent with observed spatial distributions of neritic diatoms and incorporates most processes thought to be significant regulators of diatom biomass, it can be used to elucidate mechanisms that create these temporal and spatial distributions. The magnitude of each term in equations (1) and (2) was computed and stored at monthly intervals during the simulation to indicate relative importance of all hypothesized mechanisms (*in-situ* growth, zooplankton grazing, convection, longitudinal dispersion, and exchanges between the channel and shoals) effecting population change (Figure 9). The spring period of rapid population growth in San Pablo Bay was initially (day 90) dominated by longitudinal dispersion (i.e. mixing with coastal waters assumed to have a large population density of *S. costatum*). Subsequent population growth (day 120) in the channel was maintained by a combination of *in-situ* growth, mixing with coastal waters, and inputs from the shoals where resident populations had become established and were growing rapidly [Figure 9(a),(b)]. From late spring through summer (day 150–255), biomass of *S. costatum* was maintained near steady-state in the channel because losses from grazing and longitudinal dispersion roughly balanced population gains from *in-situ* growth and transport from the shoals. Once *S. costatum* became established over the shallow areas of San Pablo Bay, its population dynamics were controlled there by a balance between rapid *in-situ* growth and loss to zooplankton (which was considerable) and transport loss to the channel [Figure 9(b)].

Although phytoplankton population dynamics have different patterns in San Pablo Bay and Suisun Bay, the development of phytoplankton populations in Suisun Bay is analogous to population development in San Pablo Bay. Note that population growth in the channel

of Suisun Bay was initiated by dispersive inputs from downstream [day 120—Figure 9(c)], and that this initial allochthonous input established *S. costatum* in waters over the shoals. During summer, *S. costatum* growth rates in the shallow areas exceeded loss rates to the channel [Figure 9(d)] and net population growth occurred in Suisun Bay. As water temperature and solar insolation declined in the fall (Figure 2), growth rates in the shallows could not match transport losses to the channel, and phytoplankton biomass became depleted in Suisun Bay. The rate of population decline was greatly accelerated by convective losses around day 285 when discharge increased dramatically during a storm [Figure 2(a)]; consequences of this convective front were also seen in eastern San Pablo Bay [note model output at station 12—Figure 8(a)].

The analysis presented in Figure 9 offers several important generalizations about population dynamics of neritic diatoms in northern San Francisco Bay. The seasonal cycle of phytoplankton population development in both San Pablo Bay and Suisun Bay is initiated by allochthonous inputs that become established over the shoals. Rapid growth there, coupled with reduced transport away from the channel in the null zone, leads to net population growth. Although Suisun and San Pablo Bays have analogous general patterns, the model has elucidated the key differences between them. First, there was a 30–60 day delay between the time populations became established in San Pablo Bay and the time at which they moved upstream to Suisun Bay [Figure 9(a),(c)]. This delay was a direct result of seasonal variations in discharge through the Sacramento–San Joaquin Rivers; note that upstream movement of *S. costatum* occurred during the period of declining discharge [Figure 2(a)]. Waters over the shoals of San Pablo Bay were apparently conducive to *S. costatum* growth during spring, since calculated growth rates were large [Figure 9(b)]. However, there was a lag between the time *S. costatum* was introduced into the shoals of Suisun Bay (day 120) and the time when calculated growth rates became significant there [day 150; Figure 9(d)]. Presumably, population growth was limited there by low salinity during early summer; calculated growth rates accelerated as discharge declined and salinity increased. Predicted growth rates were consistent with the hypothesis that light availability in the channel of San Pablo Bay was always sufficient to permit net population growth, whereas this was never the case in Suisun Bay. This suggests that all neritic diatoms in the Suisun Bay channel are derived from either the shoals or from downstream. It is informative to compare the relative importance of processes leading to population decline over the shoals. Zooplankton grazing dominated in the shoals of San Pablo Bay, while transport losses to the channel were more important in Suisun Bay [Figure 9(b),(d)]. This results from (i) higher zooplankton biomass in San Pablo Bay, and (ii) the fact that effective mixing between the shoals and channel is scaled by the lateral dimension of the shallows, and is thus slower in the larger San Pablo Bay.

One of the more valuable insights generated by this model is the observed importance of the shoals and material retention by estuarine gravitational circulation to the population development of *S. costatum* in Suisun Bay. When the model was run without these two mechanisms (i.e. by just solving the one-dimensional convection–dispersion equation), simulated population density never increased in Suisun Bay, except for a small dispersive input from San Pablo Bay during spring (Figure 10). It is possible to simulate a summer bloom in Suisun Bay without the mechanism of estuarine circulation (i.e. by simply coupling the shoals to the channel), but this requires unrealistic values for lateral exchange coefficients. It is not possible to simulate the summer bloom with the mechanism of estuarine circulation alone (i.e. by uncoupling the shoals from the channel). Although the methods used to simulate growth and transport in the shoals and, particularly, the method of handling

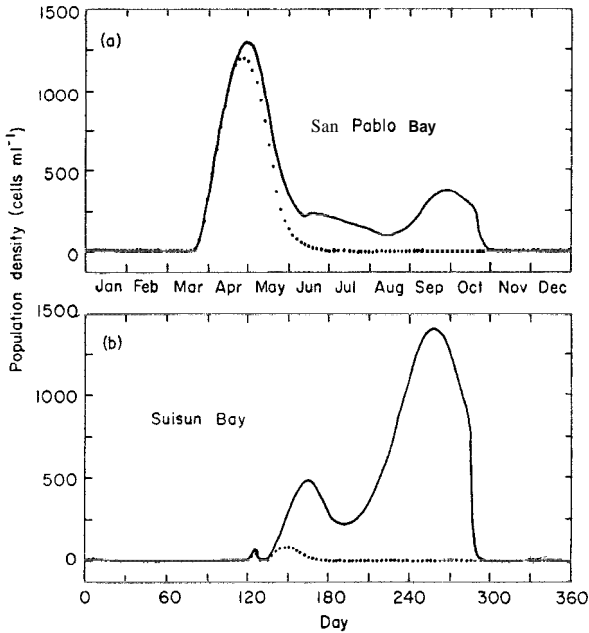


Figure 10. Comparison of simulated *S. costatum* population density in San Pablo Bay (Station 13) and Suisun Bay (Station 6) with (solid line) and without (broken line) the mechanisms of estuarine circulation and shoal-channel interactions.

estuarine circulation were only crude approximations to complex phenomena, these observations clearly demonstrate that the inclusion of both mechanisms is necessary to simulate population development of neritic phytoplankton in the landward reaches of northern San Francisco Bay.

Implications for field studies. Results of this model have stimulated a reassessment of field studies in northern San Francisco Bay. Whereas most sampling (biological and chemical constituents, salinity, temperature, etc.) has historically been concentrated in the central channel, model results suggest that phytoplankton productivity (and, hence, rates of other dynamic phenomena) is significantly greater in shallows than in the channel. Field studies are now underway to follow phytoplankton population dynamics and primary productivity in both regions. The model has also focused interest in the rate of mixing between water over the shoals and in the deeper channel.

Simulated population dynamics in San Pablo Bay were initially governed by boundary conditions [Figures 2(f), 10]. The spring bloom in San Pablo Bay was forced by assuming a large increase in *S. costatum* abundance at the seaward boundary, and this spike initiated the annual cycle of growth within the entire estuary. One mechanism that may account for this spike is the transport of neritic diatoms into San Francisco Bay from coastal water during the upwelling season. The timing and magnitude of specified boundary conditions are consistent with observations of Malone (1971) and Garrison (1976) off central California; *S. costatum* is a dominant species during the early upwelling season (February–May). On the other hand, neritic diatoms resident in the sediments of San Pablo Bay may serve as seed populations that initiate the spring bloom there. Recent evidence (Ray Wong, personal communication) suggests that viable *Skeletonema costatum* cells reside in San Pablo Bay

sediments during winter. The question of what initiates spring population development in San Pablo Bay (growth of endemic populations or allochthonous inputs) has been given added importance by the model.

Finally, the sensitivity of this model to the formulation used for quantifying zooplankton ingestion and the input values of zooplankton density stresses the need for joint studies of zooplankton and phytoplankton dynamics. We have assumed copepod densities that approximate distributions measured in 1962 and are consistent with general seasonal patterns. However, considerable errors may exist in calculated loss rates because (i) data are not sufficient to define accurately the abundance of copepods in the estuary during 1962, (ii) the complex process of phytoplankton ingestion by copepods was treated in a simple (perhaps unrealistic) manner, and (iii) grazing losses to other organisms were ignored. Simulated biomass of *S. costatum* is very sensitive to grazing losses, and realistic models are highly dependent upon accurate measures of zooplankton biomass and species composition, as well as measures of their trophic behavior (food selectivity and ingestion rates). Further, phytoplankton ingestion by organisms other than copepods (planktonic larvae of invertebrates and fish, benthic invertebrates) must be quantified before realistic systems-level models of the estuary can be developed.

Future modeling directions. This model is a simple approximation of an extremely complex ecosystem. Obviously, a predictive capability requires a more realistic treatment of the coupling between biological processes and transport processes in estuaries, but this simple model has focused attention on those mechanisms having sufficient importance to justify further refinement. Clearly, the effects of estuarine gravitational circulation on the distribution of planktonic diatoms must be given a more realistic treatment. This can be approached by using simple two-layer hydrodynamic models of the channel (e.g. Pritchard, 1969; Elliott, 1976). Or, perhaps it is necessary to couple detailed two-dimensional models of estuarine hydrodynamics (e.g. Boericke & Hogan, 1977) with settling rates and growth kinetics of phytoplankton.

While monospecific models have utility, there is a more general need for models to simulate dynamics of the entire phytoplankton assemblage. It is clear that species-specific responses to chemical and physical characteristics are important, particularly in estuaries. However, it is equally clear that separate treatment of all dominant species in a diverse assemblage is beyond the scope of most modeling needs, and is impossible because of our limited knowledge of species-specific growth kinetics. The best compromise may be to partition important phytoplankton species into a tractable number of functional groups, each of which comprises organisms having similar responses to salinity, temperature and irradiance, and whose loss rates are similar.

Conclusions

This pseudo-two-dimensional model of *S. costatum* dynamics has been useful for generating and testing hypotheses about mechanisms that regulate dynamics of neritic diatoms in northern San Francisco Bay. It suggests that seasonal changes in phytoplankton biomass within the seaward and landward reaches of the estuary channel are governed by the same general mechanism—retention of diatoms derived over shoals by estuarine circulation. However, the relative importance of biological and transport processes differ between San Pablo Bay and Suisun Bay. Future attempts to model phytoplankton dynamics in partially mixed estuaries should incorporate a realistic approximation of the transport

mechanism due to estuarine circulation, should acknowledge physiological differences within the diverse phytoplankton assemblages of estuaries, should incorporate realistic constructs of zooplankton grazing, and should consider the importance of shoals to total productivity in any system where shallows constitute a significant proportion of the total surface area.

Acknowledgements

We thank Roy A. Walters, David H. Peterson and James N. Rremer for thoughtful and constructive manuscript reviews. Richard E. Smith graciously provided meteorological, hydrological and chemical data in a useable format.

References

- Arthur, J. F. & Ball, M. D. 1979 Factors influencing the entrapment of suspended material in the San Francisco Bay-Delta estuary. In *San Francisco Bay: The Urbanized Estuary* (Conomos, T. J., ed.). Pacific Division, American Association for the Advancement of Science, San Francisco California. pp. 143-174.
- Ball, M. D. & Arthur, J. F. 1979 Planktonic chlorophyll dynamics in the northern San Francisco Bay and Delta. In *San Francisco Bay: The Urbanized Estuary* (Conomos, T. J., ed.). Pacific Division, American Association for the Advancement of Science, San Francisco, California. pp. 265-285.
- Boericke, R. R. & Hogan, J. M. 1977 An X-Z hydraulic/thermal model for estuaries. *Journal of the Hydraulics Division, Proceedings of the American Society of Civil Engineers* **103**, 19-37.
- Chapra, S. C. 1979 Applying phosphorus loading models to embayments. *Limnology and Oceanography* **24**, 163-168.
- Chen, C. W. & Orlob, G. T. 1975 Ecological simulation for aquatic environments. In *Systems Analysis and Simulation in Ecology* Vol. 3 (Patten, B. C., ed.). Academic Press, New York. pp. 476-588.
- Cloern, J. E. 1978 An empirical model of *Skeletonema costatum* photosynthetic rate, with applications in the northern San Francisco Bay estuary. *Advances in Water Resources* **1**, 267-274.
- Cloern, J. E. 1979 Phytoplankton of the San Francisco Bay system: The status of our current understanding. In *San Francisco Bay: The Urbanized Estuary* (Conomos, T. J., ed.). Pacific Division, American Association for the Advancement of Science, San Francisco, California. pp. 247-264.
- Coast and Geodetic Survey 1964 *Tidal Current Charts, San Francisco Bay*, Fifth edition. Coast and Geodetic Survey, Washington, DC.
- Cole, B. E. & Herndon, R. E. 1979 Hydrographic properties and primary productivity of San Francisco Bay waters, March 1976-July 1977. *U.S. Geological Survey Open-File Report* 79-983, 120 pp.
- Conover, R. J. 1956 Oceanography of Long Island Sound, 1952-1954. VI. Biology of *Acartia clausi* and *A. tonsa*. *Bulletin of Bingham Oceanographic Collection* 1955-6, 156-233.
- Conomos, T. J. 1979 *San Francisco Bay: The Urbanized Estuary*. Pacific Division, American Association for the Advancement of Science, San Francisco, California. 493 pp.
- Conomos, T. J. & Peterson, D. H. 1977 Suspended-particle transport and circulation in San Francisco Bay: An overview. In *Estuarine Processes* Vol. II (Wiley, M., ed.). Academic Press, New York. PP. 82-97.
- Conomos, T. J., Smith, R. E., Peterson, D. H., Hager, S. W. & Schemel, L. E. 1979 Processes affecting seasonal distributions of water properties in the San Francisco Bay system. In *San Francisco Bay: The Urbanized Estuary* (Conomos, T. J., ed.). Pacific Division, American Association for the Advancement of Science, San Francisco, California. pp. 115-142.
- DiToro, D., Thomann, R. V., O'Connor, D. J. & Mancini, J. L. 1977 Estuarine phytoplankton biomass models-verification analyses and preliminary applications. In *The Sea* Vol. 6 (Goldberg, E. D., McCave, I. N., O'Brien, J. J. & Steele, J. H., eds). Wiley-Interscience, New York. pp. 969-1020.
- Elliott, A. J. 1976 A mixed-dimension kinematic estuarine model. *Chesapeake Science* **17**, 135-140.
- Eppley, R. W. & Sloan, P. R. 1965 Carbon balance experiments with marine phytoplankton. *Journal of the Fisheries Research Board of Canada* **22**, 1083-1097.
- Garrison, D. L. 1976 Contribution of the net plankton and nanoplankton to the standing stocks and primary productivity in Monterey Bay, California during the upwelling season. *Fisheries Bulletin* **74**, 183-194.
- Glennie, B. & Selleck, R. E. 1969 Longitudinal estuarine diffusion in San Francisco Bay, California. *Water Research* **3**, 1-20.
- Harleman, D. R. F. 1971 One-dimensional models. In *Estuarine Modeling: An Assessment*. Environmental Protection Agency, Water Quality Office Research Report 16070DZW. pp. 34-89.
- Jorgensen, E. G. 1968 The adaptation of plankton algae. II, Aspects of the temperature adaptation of *Skeletonema costatum*. *Plant Physiology* **21**, 423-427.

- Kelley, R. A. 1976 Conceptual ecological model of the Delaware Estuary. In *Systems Analysis and Simulation in Ecology* Vol. 4 (Patten, B. C., ed.). Academic Press, New York. pp. 3-46.
- Ketchum, B. H. 1950 Hydrographic factors involved in the dispersion of pollutants introduced into tidal waters. *Journal of the Boston Society of Civil Engineers* 37, 296-314.
- McAllister, C. D., Shah, N. & Strickland, J. D. H. 1964 Marine phytoplankton photosynthesis as a function of light intensity: A comparison of methods. *Journal of the Fisheries Research Board of Canada* 21, 159-181.
- McCracken, D. D. & Dorn, W. S. 1964 *Numerical Methods and FORTRAN Programming*. John Wiley and Sons, Inc., New York, 457 pp.
- Malone, T. C. 1971 The relative importance of nanoplankton and netplankton as primary producers in the California current system. *Fisheries Bulletin* 69, 799-820.
- Meade, R. H. 1972 Transport and deposition of sediments in estuaries. *Geological Society of America Memoires* 133, 91-120.
- Xival, P. & Nival, S. 1976 Particle retention efficiencies of an herbivorous copepod, *Acartia claus* (adult and copepodite stages); effects on grazing. *Limnology and Oceanography* 21, 24-38.
- O'Connors, H. B., Small, L. F. & Donaghay, P. L. 1976 Particle-size modification by two size classes of the estuarine copepod *Acartia clausi*. *Limnology and Oceanography* 21, 300-308.
- Painter, R. E. 1966 Zooplankton of San Pablo and Suisun Bays. *California Department of Fish and Game, Fisheries Bulletin* 133, 18-39.
- Peterson, D. H. & Conomos, T. J. 1975 Implications of seasonal chemical and physical factors on the production of phytoplankton in northern San Francisco Bay. In *Proceedings of a Workshop on Algae Nutrient Relationships in the San Francisco Bay and Delta (8-10 November 1973)* (Brown, R. L., ed.). The San Francisco Bay and Estuarine Association, San Francisco, California. pp. 147-185.
- Peterson, D. H., Conomos, T. J., Broenkow, W. W. & Scrivani, E. P. 1975a Processes controlling the dissolved silica distribution in San Francisco Bay. In *Estuarine Research* Vol. 1 (Cronin, L. E., ed.). Academic Press, New York. pp. 153-187.
- Peterson, D. H., Conomos, T. J., Broenkow, W. W. & Doherty, P. C. 1975b Location of the nontidal current null zone in northern San Francisco Bay. *Estuarine and Coastal Marine Science* 3, 1-11.
- Postma, H. 1967 Sediment transport and sedimentation in the estuarine environment. In *Estuaries* (Lauff, G. H., ed.). Science Publication 83, Washington, D.C. pp. 158-179.
- Pritchard, D. W. 1969 Dispersion and flushing of pollutants in estuaries. *Journal of the Hydraulics Division, Proceedings of the American Society of Civil Engineers* 95, 115-124.
- Richman, S., Heinle, D. R. & Huff, R. 1977 Grazing by adult estuarine calanoid copepods of the Chesapeake Bay. *Marine Biology* 42, 69-84.
- Smith, R. E., Herndon, R. E. & Harmon, D. D. 1979 Physical and chemical properties of San Francisco Bay waters, 1969-1976. *U.S. Geological Survey Open-File Report 79-511*. 607 pp.
- Steele, J. H. 196j Notes on some theoretical problems in production ecology, pp. 383-398. In *Primary Productivity in Aquatic Environments* (Goldman, C. R., ed.). *Memorie dell'Istituto Italiano di Idrobiologia* 18 (Supplement), University of California Press, Berkeley.
- Stevens, D. E. 1979 Environmental factors affecting striped bass (*Morone saxatilis*) in the Sacramento-San Joaquin Estuary. In *San Francisco Bay: The Urbanized Estuary* (Conomos, T. J., ed.). Pacific Division, American Association for the Advancement of Science, San Francisco, California. pp. 469-478.
- Storrs, P. N., Selleck, R. E. & Pearson, E. A. 1963 A comprehensive study of San Francisco Bay, 1961-1962. *University of California Sanitary Engineering Research Laboratory, Report No. 63-3*. Berkeley, California. 221 pp.
- Storrs, P. N., Selleck, R. E. & Pearson, E. A. 1964 A comprehensive study of San Francisco Bay, 1963-64. *University of California Sanitary Engineering Research Laboratory, Report No. 64-4* (Appendix). Berkeley, California.
- Storrs, P. N., Pearson, E. A. & Selleck, R. E. 1966 A comprehensive study of San Francisco Bay, Vol. V. *University of California Sanitary Engineering Research Laboratory, Report No. 67-2*. Berkeley, California. 139 pp.
- U.S. Bureau of Reclamation. 1976 *Delta-Suisun Bay Ecological Studies. A Report of Water Quality in the Sacramento-San Joaquin Estuary during the Low Flow Year, 1976*. USBK, Water Quality Branch, Sacramento, California. 227 pp.
- U.S. Bureau of Reclamation, California Department of Water Resources and California Department of Fish and Game. 1977 *Delta-Suisun Bay ecological studies. Biological methods and data for 1968-1974*. USBR Water Quality Branch, Sacramento, California. 592 pp.
- Vollenweider, R. A. 1965 Calculation models of photosynthesis-depth curves and some implications regarding day rate estimates in primary production estimates. In *Primary Productivity in Aquatic Environments* (Goldman, C. R., ed.). *Memorie dell'Istituto Italiano di Idrobiologia* 18 (Supplement), University of California Press, Berkeley. pp. 425-457.
- Walters, R. A. & Cheng, R. T. 1979 A two-dimensional hydrodynamic model of a tidal estuary. *Advances in Water Resources* 2, 177-184.